Ca^{2+} and synaptotagmin VII–dependent delivery of lysosomal membrane to nascent phagosomes

Cecilia Czibener,[1] Nathan M. Sherer,[1] Steven M. Becker,[1] Marc Pypaert,[2] Enfu Hui,[3,4] Edwin R. Chapman,[3,4] Walther Mothes,[1] and Norma W. Andrews[1,2]

[1]Section of Microbial Pathogenesis and [2]Department of Cell Biology, Yale University School of Medicine, New Haven, CT 06510
[3]Howard Hughes Medical Institute and [4]Department of Physiology, University of Wisconsin, Madison, WI 53706

Synaptotagmin (Syt) VII is a ubiquitously expressed member of the Syt family of Ca^{2+} sensors. It is present on lysosomes in several cell types, where it regulates Ca^{2+}-dependent exocytosis. Because $[Ca^{2+}]_i$ and exocytosis have been associated with phagocytosis, we investigated the phagocytic ability of macrophages from Syt $VII^{-/-}$ mice. Syt $VII^{-/-}$ macrophages phagocytose normally at low particle/cell ratios but show a progressive inhibition in particle uptake under high load conditions. Complementation with Syt VII rescues this phenotype, but only when functional Ca^{2+}-binding sites are retained. Reinforcing a role for Syt VII in Ca^{2+}-dependent phagocytosis, particle uptake in Syt $VII^{-/-}$ macrophages is significantly less dependent on $[Ca^{2+}]_i$. Syt VII is concentrated on peripheral domains of lysosomal compartments, from where it is recruited to nascent phagosomes. Syt VII recruitment is rapidly followed by the delivery of Lamp1 to phagosomes, a process that is inhibited in Syt $VII^{-/-}$ macrophages. Thus, Syt VII regulates the Ca^{2+}-dependent mobilization of lysosomes as a supplemental source of membrane during phagocytosis.

Introduction

Phagocytosis is the process by which cells internalize large particles of >0.5 μm in diameter. Most bacterial, fungal, and protozoan pathogens fall within this size range, and phagocytosis by macrophages, dendritic cells, and neutrophils is critical for the clearance of these organisms from infected mammals. Phagocytosis also plays a key role in the removal of dead cells and in the induction of tolerance or initiation of immune responses. Particle uptake is induced by the ligation of specific receptors on the surface of phagocytes, which trigger a membrane remodeling process that is largely dependent on actin polymerization. Depending on the receptors used, distinct signaling pathways are activated, and the engulfment pattern can vary from extensive pseudopod extension to an inward movement of the particle in a sinking fashion (Aderem and Underhill, 1999; Greenberg and Grinstein, 2002).

Early studies of phagocytosis in macrophages concluded that the phagosome was formed largely by invaginated plasma membrane (Werb and Cohn, 1972; Silverstein et al., 1977). Later studies found a transient increase in surface area during the early stages of particle uptake (Hackam et al., 1998; Holevinsky and Nelson, 1998) or after plating macrophages on immobilized IgG (Cox et al., 1999), suggesting that membrane from an intracellular source was inserted by exocytosis. This intracellular source of membrane was first identified as early endosomes (Bajno et al., 2000; Cox et al., 2000; Niedergang et al., 2003), and, more recently, late endosomes were also implicated (Braun et al., 2004). The functional inhibition of tetanus neurotoxin–insensitive vesicle-associated membrane protein (VAMP)/VAMP7, a late endosome/lysosome v-SNARE (Advani et al., 1998, 1999), inhibited IgG or complement-mediated particle uptake (Braun et al., 2004). Fusion of lysosomes with the plasma membrane was detected during the early stages of particle uptake (Braun et al., 2004), which is consistent with earlier observations of lysosomal enzyme release by macrophages during phagocytosis (Werb and Gordon, 1975; Leoni and Dean, 1983; Tapper and Sundler, 1995).

The identification of synaptotagmin (Syt) VII as a regulator of lysosomal exocytosis (Martinez et al., 2000; Reddy et al., 2001; Roy et al., 2004) prompted us to investigate its possible role in phagocytosis. Syts belong to a large family of membrane proteins characterized by the presence of two Ca^{2+}-binding C2 domains on their cytoplasmic region (Chapman, 2002). Syts I and VII, two evolutionally conserved members of the family,

Correspondence to Norma W. Andrews: norma.andrews@yale.edu

Abbreviations used in this paper: BMM, bone marrow macrophage; PC, phosphatidylcholine; PS, phosphatidylserine; Syt, synaptotagmin; VAMP, vesicle-associated membrane protein.

The online version of this article contains supplemental material.

© The Rockefeller University Press $8.00
The Journal of Cell Biology, Vol. 174, No. 7, September 25, 2006 997–1007
http://www.jcb.org/cgi/doi/10.1083/jcb.200605004

are thought to promote membrane fusion by functioning as exocytic Ca^{2+} sensors of low and high affinity, respectively (Bhalla et al., 2005). Syt I controls synaptic vesicle exocytosis in neurons (Chapman, 2002; Koh and Bellen, 2003), and Syt VII regulates the secretion of lysosomes (Martinez et al., 2000) and of some nonsynaptic secretory granules of specialized cells (Gao et al., 2000; Fukuda et al., 2004; Wang et al., 2005). In this study, by examining the phagocytic ability of macrophages from Syt $VII^{-/-}$ mice (Chakrabarti et al., 2003), we clarify a long-standing controversy about the role of intracellular free Ca^{2+} ($[Ca^{2+}]_i$) in phagocytosis. Previous studies, which were performed under different conditions, arrived at contradictory conclusions regarding the requirement for $[Ca^{2+}]_i$ transients in phagocytosis (Young et al., 1984; McNeil et al., 1986; Di Virgilio et al., 1988; Greenberg et al., 1991; Hishikawa et al., 1991). Our results indicate that $[Ca^{2+}]_i$ is preferentially required for a Syt VII–dependent component of the phagocytic process, which involves the delivery of lysosomal membrane to nascent phagosomes. Imaging analysis revealed that Syt VII–containing domains of lysosomal compartments are rapidly mobilized to phagosomes and to ruffling regions of the plasma membrane, facilitating the uptake of large particle loads.

Results

Syt $VII^{-/-}$ bone marrow macrophages are impaired in phagocytosis, and the defect increases with the particle load

Dominant-negative constructs or RNAi silencing of the late endosomal/lysosomal v-SNARE VAMP7 inhibit particle uptake by RAW267.7 macrophages (Braun et al., 2004), suggesting that lysosomal fusion is required for some forms of phagocytosis. To further understand this process, we investigated the role of Syt VII, the Ca^{2+}-binding membrane protein that was previously shown to regulate the fusion of lysosomes with the plasma membrane (Martinez et al., 2000). Bone marrow macrophages (BMMs) from Syt $VII^{+/+}$ or $VII^{-/-}$ mice were exposed to IgG-opsonized fluorescent zymosan particles at different particle/cell ratios for increasing periods of time. Fluorescence microscopy examination suggested that uptake was reduced in Syt$VII^{-/-}$ BMMs, particularly at later time points (Fig. 1 A). This was confirmed by measuring the fluorescence associated with BMMs in a fluorimeter: as the particle/cell ratio increased, defective particle uptake became evident in Syt $VII^{-/-}$ BMMs (Fig. 1 B). The phagocytosis defect increased with time, suggesting that Syt VII is required for the continuous uptake of large particle loads.

A previous study revealed no difference in the uptake of *Escherichia coli*, *Listeria monocytogenes*, *Yersinia pseudotuberculosis*, and *Salmonella typhimurium* by Syt $VII^{+/+}$ or $VII^{-/-}$ BMMs (Roy et al., 2004). This suggested that the defective phagocytosis of zymosan might be related to their larger size (4–5 μm) when compared with bacteria (0.5–2 μm). To directly investigate this possibility, we exposed BMMs to 3- or 6-μm fluorescent latex beads and determined the number of phagocytosed particles after increasing periods of time. The uptake of 3-μm beads was nearly identical for both groups of BMMs except for a small inhibition detected after 1 h in Syt $VII^{-/-}$ BMMs at the highest particle/cell ratio. In contrast, phagocytosis of 6-μm beads was reduced in Syt $VII^{-/-}$ BMMs at all time points at both 10 and 25 particles/cell (Fig. 1 C). This phenotype was independent of the receptor-mediating particle uptake; impaired

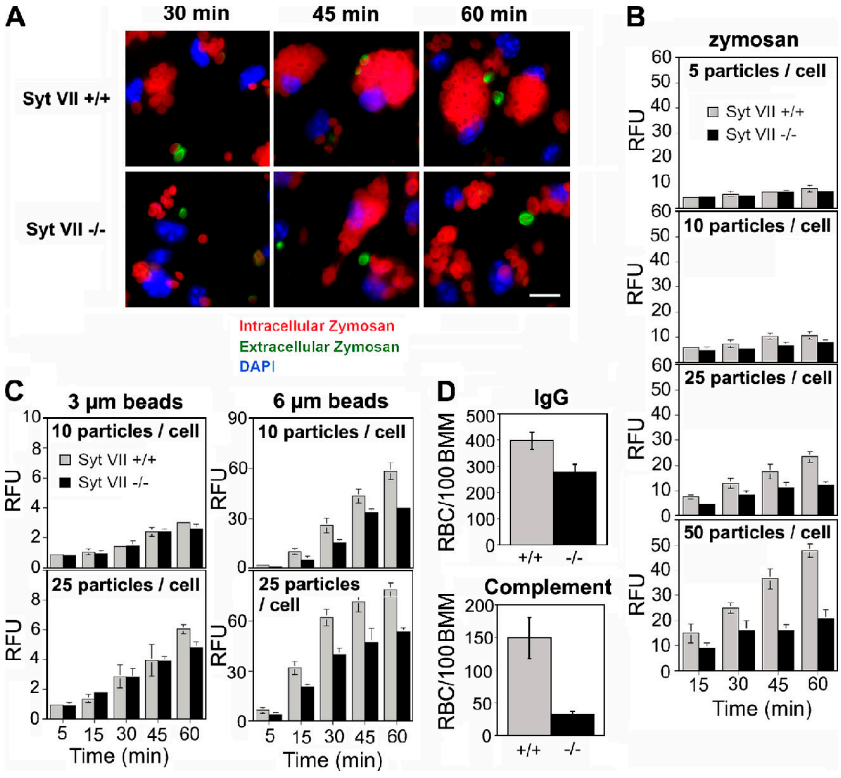

Figure 1. **The phagocytosis defect of Syt $VII^{-/-}$ BMMs increases with particle load and size.** (A) Syt $VII^{+/+}$ or $VII^{-/-}$ BMMs were exposed to 25 IgG-opsonized zymosan red particles/cell for the periods of time indicated. Cells were washed, fixed, and stained without permeabilization to detect extracellular particles (green) and nuclei (DAPI, blue). Bar, 10 μm. (B) The phagocytosis defect of Syt $VII^{-/-}$ BMMs increases with particle load. Opsonized zymosan red uptake was determined fluorometrically at the indicated time points after incubation with increasing numbers of particles/cell. (C) The phagocytosis defect of Syt $VII^{-/-}$ BMMs increases with particle size. The uptake of IgG-opsonized fluorescent polystyrene particles was determined fluorometrically at the indicated time points after incubation with 10 or 25 particles/cell. RFU, relative fluorescence unit. (D) The uptake defect of Syt $VII^{-/-}$ BMMs is independent of the receptor-mediating phagocytosis. The number of internalized sheep RBCs opsonized with IgG or complement was determined after BMM exposure to 10 particles/cell for 30 min. The data represent the mean ± SD (error bars) of triplicates.

phagocytosis in Syt VII$^{-/-}$ BMMs was observed when assays were performed with nonopsonized zymosan (not depicted) or with sheep RBCs opsonized with either IgG or complement (Fig. 1 D). The phagocytosis defect was not related to a reduced expression of surface receptors because flow cytometry detected similar levels of FcγR or CR3 (Cd11b) on Syt VII$^{+/+}$ or VII$^{-/-}$ BMMs (Fig. S1, available at http://www.jcb.org/cgi/content/full/jcb.200605004/DC1).

Syt VII is required for a Ca^{2+}-dependent component of phagocytosis

The aforementioned results suggested that Syt VII might facilitate the uptake of large particle loads by mediating the Ca^{2+}-dependent delivery of intracellular membranes to phagosomes. This hypothesis predicts that phagocytosis in Syt VII$^{-/-}$ BMMs should be less sensitive to $[Ca^{2+}]_i$ chelation when compared with wild type. To investigate this possibility, BMMs from Syt VII$^{+/+}$ or VII$^{-/-}$ mice were pretreated or not treated with the membrane-permeant Ca^{2+} chelator BAPTA-AM and exposed to IgG-opsonized zymosan particles for increasing periods of time. In Syt VII$^{+/+}$ BMMs, BAPTA inhibited particle uptake by 66–84% (Fig. 2 A). In contrast, $[Ca^{2+}]_i$ chelation in Syt VII$^{-/-}$ BMMs did not inhibit uptake at the early time points, and, after longer incubation periods, phagocytosis was only reduced by 30–37% (Fig. 2 B). Thus, $[Ca^{2+}]_i$ appeared to be preferentially required for a Syt VII–dependent component of the particle uptake process.

To directly assess the importance of Syt VII Ca^{2+}-binding activity in phagocytosis, we performed functional reconstitution experiments in Syt VII$^{-/-}$ BMMs. The macrophages were retrovirally transduced with wild-type Syt VII–YFP, YFP alone, or a full-length Syt VII–YFP construct in which the four aspartic acid residues predicted to be involved in Ca^{2+} binding (Li et al., 1995; Bhalla et al., 2005) were mutated to asparagines (Syt VII (D/N)–YFP). After exposure to zymosan particles for 1 h, Syt VII$^{-/-}$ BMMs were fixed, and the number of internalized particles was quantified microscopically on transduced YFP-expressing cells. In several independent experiments, wild-type Syt VII–YFP markedly enhanced particle uptake when compared with BMMs expressing YFP alone. In contrast, when the putative Ca^{2+}-binding sites of the C2A and C2B domains were mutated (D225N-D227N and D357N-D359N mutations), the ability of Syt VII to restore normal levels of phagocytosis was abolished (Fig. 2 C). Syt VII–YFP and Syt VII (D/N)–YFP were expressed at similar levels and were localized on tubulovesicular intracellular compartments of Syt VII$^{-/-}$ BMMs (Fig. 2 D). However, only Syt VII–YFP was clearly detected on the membrane of most zymosan-containing phagosomes (Fig. 2 D, top). In contrast, Syt VII (D/N)–YFP did not appear to be efficiently delivered to the few phagosomes present in Syt VII$^{-/-}$ BMMs expressing this construct (Fig. 2 D, bottom).

Mutations in the predicted Ca^{2+}-binding sites of the major neuronal Syt isoform Syt I (D230N-D232N and D363N-D365N, respectively) abolish its interaction with phosphatidylserine (PS; Earles et al., 2001) and disrupt Ca^{2+}-regulated SNARE-mediated membrane fusion in vitro (Tucker et al., 2004; Bhalla et al., 2006). The effect of equivalent mutations on the Syt VII C2A (D225N-D227N) and C2B domains (D357N-D359N) had not yet been examined, so we performed binding assays using PS/phosphatidylcholine (PC) liposomes and immobilized Syts I and VII C2AB fragments. As expected (Bhalla et al., 2005), Ca^{2+}-dependent PS-binding activity was observed for both Syt isoforms (Fig. 2 E). However, when the putative Ca^{2+}-binding ligands of C2AB VII were neutralized (D/N mutations), we observed marked Ca^{2+}-independent binding to PS/PC liposomes.

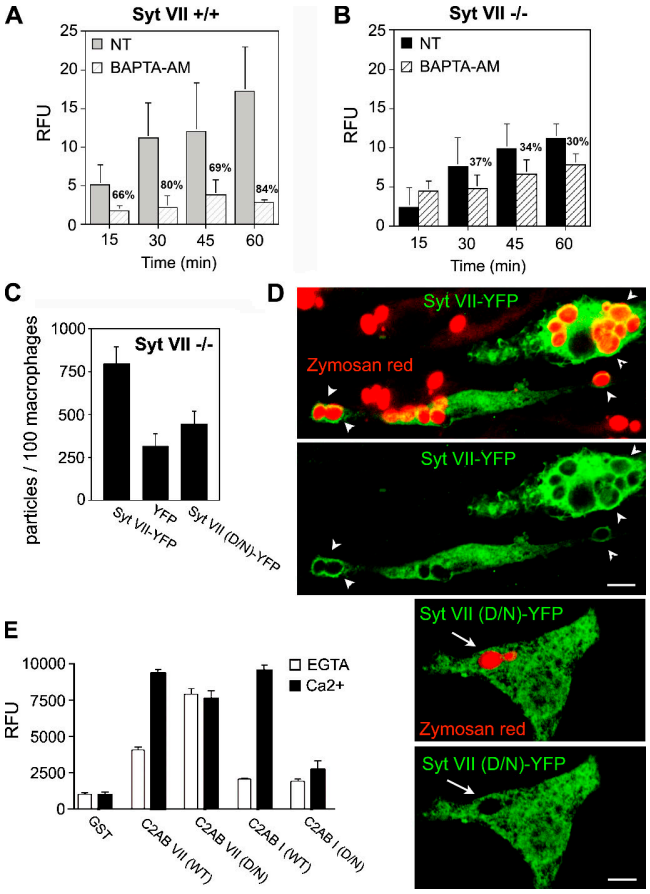

Figure 2. **Ca^{2+}-dependent Syt VII activity regulates phagocytosis.** (A and B) Residual phagocytosis of Syt VII$^{-/-}$ BMMs is less dependent on $[Ca^{2+}]_i$. BMMs pretreated or not treated (NT) with BAPTA-AM were exposed to 10 IgG-opsonized zymosan red/cell. After the indicated time points, cells were washed, fixed, and the number of internalized particles were determined fluorometrically. (A) Syt VII$^{+/+}$ BMMs. (B) Syt VII$^{-/-}$ BMMs. Percent inhibition for each time point is indicated. (C) Syt VII–YFP restores phagocytosis to wild-type levels. Syt VII$^{-/-}$ BMMs were transduced with Syt VII–YFP, YFP, or Syt VII (D/N)–YFP (full-length Syt VII with mutations on the four putative Ca^{2+}-binding residues) and exposed to 25 IgG-opsonized zymosan red/cell for 1 h. (D) Syt VII (D/N)–YFP is not recruited to phagosomes as efficiently as Syt VII–YFP. Confocal images of the BMMs in C, acquired under identical conditions. Both constructs were targeted to tubular intracellular compartments, but only Syt VII–YFP was efficiently recruited to zymosan red–containing phagosomes (arrowheads, top). Arrows in the bottom panels point to Syt VII (D/N)–YFP-negative phagosomes. The YFP signal was enhanced by immunofluorescence with anti-GFP antibodies. Bars, 5 μm. (E) Mutations in the predicted Ca^{2+}-binding residues shift the PS binding of C2AB VII from Ca^{2+} dependent to Ca^{2+} independent. The binding of GST–C2AB VII, GST–C2AB VII (D/N), GST–C2AB I, and GST–C2AB I (D/N) to PS-containing liposomes was determined. Proteins were immobilized on glutathione–Sepharose beads and assayed for the binding of PS/PC liposomes in the presence of 2 mM EGTA (white bars) or 0.2 mM Ca^{2+} (black bars). RFU, relative fluorescence unit. The data represent the mean ± SD (error bars) of triplicates.

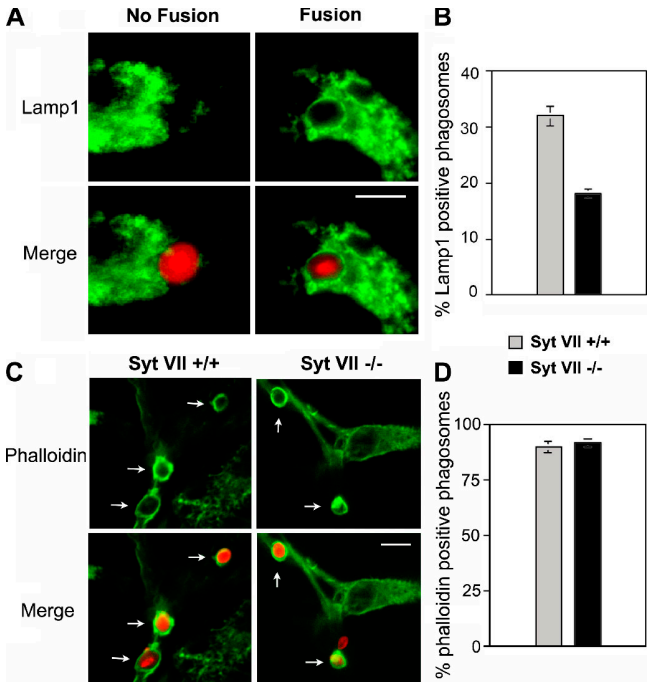

Figure 3. **The early fusion of lysosomes with phagosomes is impaired in Syt VII$^{-/-}$ BMMs.** BMMs were exposed to opsonized zymosan red for 10 min, fixed, and stained with anti-Lamp1 mAbs (A and B) or phalloidin (C and D). (A) Examples of the morphological criteria used to score phagosomes for fusion or no fusion. (B) Percentage of phagosomes that fused with Lamp1-containing lysosomes. (C) Images of phalloidin-stained recently formed phagosomes in Syt VII$^{+/+}$ or VI$^{-/-}$ BMMs. The arrows point to phagosomes containing zymosan red surrounded by phalloidin-stained polymerized actin. (D) Percentage of phalloidin-positive phagosomes. (B and D) The data represent the mean ± SD (error bars) of triplicates. Bars, 5 μm.

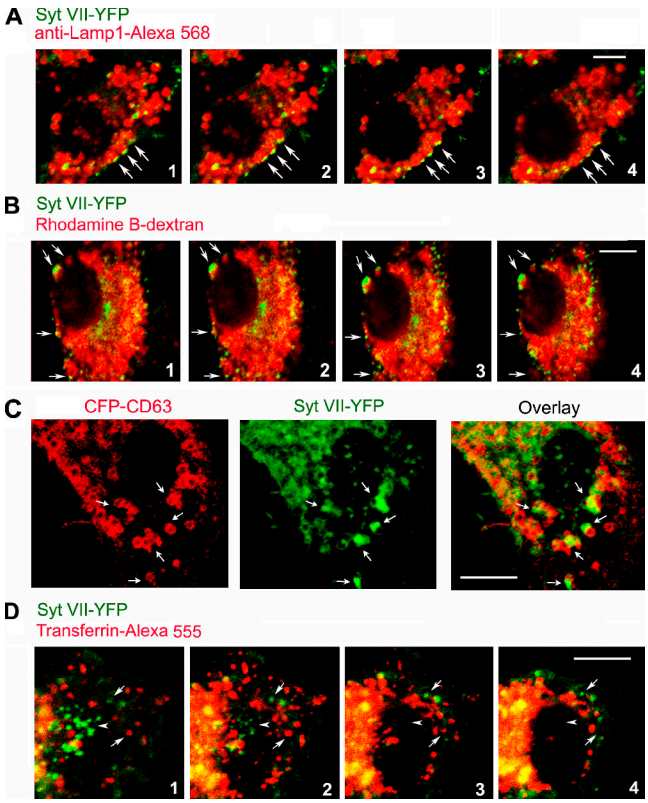

Figure 4. **Syt VII–YFP colocalizes with peripheral domains of late endosomes/lysosomes.** (A) BMMs were transduced with Syt VII–YFP, fixed, and stained with anti-Lamp1 mAbs. (B) BMMs were transduced with Syt VII–YFP, and the lysosomal compartment was loaded with rhodamine B–dextran before fixation. (A and B) Images are sequential 0.8-μm optical slices of a confocal z stack. (C) BMMs were transduced with Syt VII–YFP and CFP-CD63 and examined by live confocal microscopy. (A–C) The arrows point to domains enriched in Syt VII–YFP that were closely associated with Lamp1-positive compartments (A), rhodamine B–dextran-containing compartments (B), or compartments containing CFP-CD63 (C). (D) BMMs were transduced with Syt VII–YFP, and early endosomes were loaded with AlexaFluor555-transferrin before fixation. Images are sequential 0.8-μm optical slices of a confocal z stack. Arrows point to compartments containing Syt VII–YFP or AlexaFluor555-transferrin that are not in close association with each other. Arrowheads point to a cluster of Syt VII–enriched domains that are not associated with transferrin-containing early endosomes. Bars, 5 μm.

Similar constructs carrying equivalent mutations in the Syt I Ca^{2+} ligands abolished Ca^{2+}-triggered binding to PS/PC liposomes, which is consistent with previous experiments (Earles et al., 2001). Thus, Ca^{2+} ligand mutations in both Syts I and VII abolish Ca^{2+}-regulated interactions with PS, but, in the case of Syt VII, the PS-binding activity is rendered constitutive. Because Syt VII (D/N) fails to rescue phagocytosis, this Ca^{2+}-independent PS-binding activity does not appear to influence membrane traffic events leading to phagosome formation.

PS is an essential effector of Syts I, IX, and VII during regulated membrane fusion (Bhalla et al., 2005), and the Ca^{2+} ligand mutations in Syt VII affect this activity. It is conceivable that the constitutive lipid-binding activity of Syt VII (D/N) causes the binding of the C2 domains to the lysosomal membrane (e.g., the cis membrane to which the protein is anchored via its transmembrane domain) rather than to the target membrane (i.e., interacting with the plasma membrane in response to a rise in intracellular Ca^{2+}), preventing Syt from engaging the target membrane and, thus, failing to stimulate fusion. The D/N mutations may also impair Ca^{2+}-dependent Syt VII–t-SNARE interactions, resulting in a failure to activate t-SNAREs for fusion (Tucker et al., 2004). In any case, our data demonstrate that the Ca^{2+} ligand mutations disrupt the ability of Ca^{2+} to regulate the interaction of Syt VII with an essential effector, PS, resulting in a failure to restore normal phagocytosis in Syt VII$^{-/-}$ BMMs.

Early recruitment of Lamp1 to phagosomes is inhibited in Syt VII$^{-/-}$ BMMs

In several cell types, Syt VII colocalizes with lysosomal markers and regulates lysosome fusion with the plasma membrane (Martinez et al., 2000; Caler et al., 2001; Reddy et al., 2001; Chakrabarti et al., 2003). When expressed in Syt VII–deficient BMMs, Syt VII–YFP restored phagocytosis to wild-type levels and was detected on the membrane of phagosomes (Fig. 2). Collectively, these findings suggested that Syt VII might facilitate the uptake of large particle loads by regulating lysosomal membrane delivery to phagosomes. To test this hypothesis, BMMs from Syt VII$^{+/+}$ or VII$^{-/-}$ mice were exposed to zymosan for 10 min, fixed, and stained with antibodies against the major lysosomal glycoprotein Lamp1. These experiments were performed at a particle/BMM ratio of 10, a condition that allows the formation of a similar number of phagosomes in Syt VII$^{+/+}$ and VII$^{-/-}$ BMMs (Fig. 1 B).

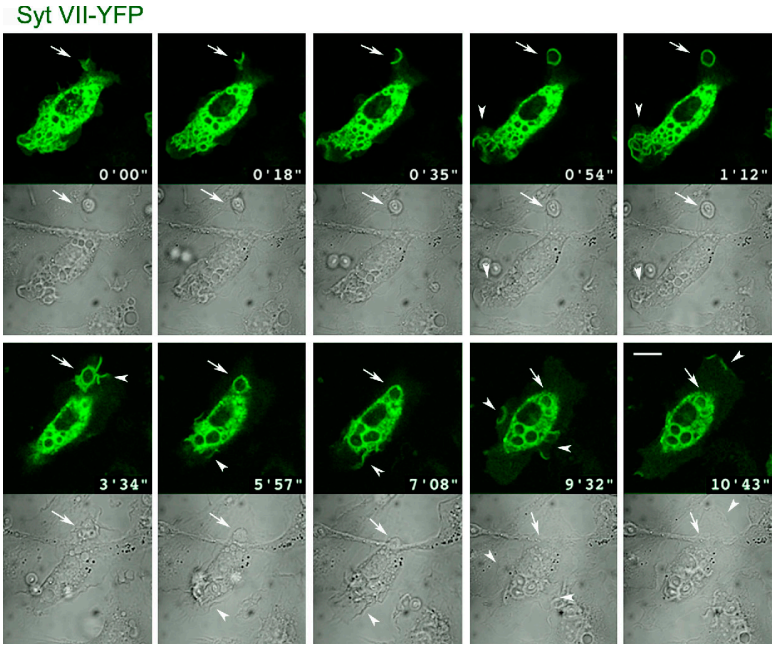

Figure 5. **Syt VII–YFP is rapidly recruited to phagocytic cups and to nascent phagosomes.** Selected frames from a confocal time-lapse video of a BMM transduced with Syt VII–YFP and exposed to 10 IgG-opsonized zymosan particles/cell (Video 1, available at http://www.jcb.org/cgi/content/full/jcb.200605004/DC1). The images show the rapid recruitment of Syt VII–YFP to sites of particle attachment and to expanding phagocytic cups (arrows). At later time points, Syt VII–YFP recruitment is also detected on areas of plasma membrane ruffling, which were associated (frames at 1 min 12 s and at 3 min 34 s) or not associated (frames at 9 min 32 s and at 10 min 43 s) with particle uptake (arrowheads). Top panels, YFP channel; bottom panels, differential interference contrast. Bar, 10 μm.

Equivalent numbers of phagosomes (>200) were scored in both groups of BMMs for the presence or absence of defined Lamp1 staining on phagosome membranes (Fig. 3 A). The results revealed a marked reduction in the number of Lamp1-positive phagosomes in Syt VII$^{-/-}$ BMMs. After 10 min, 32% of recently formed phagosomes in Syt VII$^{+/+}$ BMMs were Lamp1 positive, whereas in Syt VII$^{-/-}$ BMMs, only 18% stained positive (Fig. 3 B). These results are consistent with a previous study describing the detection of the lysosomal v-SNARE VAMP7 on ~40% of recently formed phagosomes in RAW264.7 macrophages (Braun et al., 2004). The large majority of the phagosomes within Syt VII$^{+/+}$ or VII$^{-/-}$ BMMs (89.6 and 92.2%, respectively) were still heavily surrounded by polymerized actin after the 10-min incubation period (Fig. 3, C and D), indicating that the reduced Lamp1 staining in Syt VII$^{-/-}$ BMMs was not a result of a slower rate of phagosome maturation (Lang et al., 1988; Desjardins et al., 1994). Reinforcing this view, specific labeling for Lamp1 was detected by cryoimmuno-EM on the membrane of recently formed phagosomes that were still at the cell periphery, which is in close proximity to ruffling areas of the plasma membrane (Fig. S2, available at http://www.jcb.org/cgi/content/full/jcb.200605004/DC1).

Syt VII is concentrated on peripheral domains of lysosomal compartments

Retroviral expression of Syt VII–YFP restores phagocytosis in Syt VII$^{-/-}$ BMMs to wild-type levels (Fig. 2 C), demonstrating that this construct is fully functional. Similarly tagged Syt VII constructs were previously shown to colocalize with endogenous lysosomal markers in the cell lines NRK (Martinez et al., 2000), CHO (Jaiswal et al., 2002), and PC12 (Fukuda et al., 2004; Wang et al., 2005) as well as in primary keratinocytes (Hakansson et al., 2005). Consistent with these earlier studies, Syt VII–YFP expressed in BMMs was detected in association with Lamp1-positive late endosomes/lysosomes. Interestingly, confocal z optical sectioning revealed higher concentrations of Syt VII on peripheral regions of Lamp1-positive compartments (Fig. 4 A). On sequential optical sections, Syt VII–enriched domains were consistently observed in close association with the Lamp1-containing late endosomes/lysosomes in a defined cap pattern oriented toward the plasma membrane (Fig. 4 A). A similar pattern was observed when the lysosomal compartments of Syt VII–YFP-transduced BMMs were loaded with rhodamine B–dextran by endocytosis followed by a 2-h chase period (Fig. 4 B). BMMs were also doubly transduced with Syt VII–YFP and CFP-CD63, a tetraspanin used extensively as a marker of late endosomes and lysosomes (Duffield et al., 2003; Pelchen-Matthews et al., 2003). Syt VII–YFP was again detected in defined microdomains, which were closely associated with tubulovesicular compartments containing CFP-CD63 (Fig. 4 C). In contrast, the Syt VII–YFP-enriched membrane domains were not closely associated with transferrin-containing early endosomes (Fig. 4 D).

Syt VII and Lamp1-containing membranes are sequentially recruited to nascent phagosomes

To further investigate the apparent delivery of Syt VII to phagosomes (Fig. 2 D), we performed time-lapse confocal microscopy of live BMMs during the particle uptake process. We found that Syt VII–YFP was recruited to sites of phagosome formation during early steps of the process immediately after binding of the particle to the macrophage surface (Fig. 5 and Video 1, available at http://www.jcb.org/cgi/content/full/jcb.200605004/DC1). A few seconds after the contact of opsonized zymosan with the membrane of BMMs, the Syt VII–YFP fluorescent signal became very intense at the base of nascent phagosomes. This signal persisted during formation of the phagocytic cup and progressed to completely surround the particles (Fig. 5 and Video 1, frames from 0 min 18 s to 0 min 54 s).

Interestingly, Syt VII delivery to the plasma membrane was also observed at the sites of intense membrane ruffling that follow phagocytic cup closure, leading to particle engulfment. Syt VII–YFP was also detected at sites of plasma membrane ruffling that were not associated with phagocytosis (Fig. 5 and Video 1, frames from 1 min 12 s to 10 min 43 s).

These observations suggested that Syt VII was recruited to nascent phagocytic cups from the peripheral domains of lysosomal compartments, where the protein is localized in resting BMMs. Such a scenario would predict that additional lysosomal resident proteins such as Lamp1 should also be detected on nascent or recently formed phagosomes. To investigate this issue, wide-field time-lapse fluorescence microscopy was performed in live BMMs transduced with Syt VII–YFP and Lamp1-RFP. Lamp1-RFP was detected throughout the dense perinuclear portions of the lysosomal compartment and also on clearly defined tubules extending toward the cell periphery. These dynamic peripheral tubules also contained Syt VII–YFP (Fig. 6 A, insets of frame at 3 min 12 s). Shortly after Syt VII was visualized colocalizing with Lamp1 on the peripheral tubules, it appeared on the membrane of nascent phagocytic cups (Fig. 6 A, frames from 3 min 12 s to 10 min 24 s; and Videos 2–4, available at http://www.jcb.org/cgi/content/full/jcb.200605004/DC1). Lamp1-containing tubules were initially visualized as a scaffold at the site where Syt VII accumulated, before formation of the phagocytic cup. Immediately after this initial step, Lamp1-positive tubules were observed wrapping themselves around Syt VII–positive nascent phagocytic cups (Fig. 6 A and Videos 2–4). A very similar process was observed during the formation of macropinosomes (Videos 2 and 3).

Confocal microscopy confirmed the close association of Lamp1 with Syt VII on nascent phagosomes (Fig. 6 B, boxed area 1) and their full colocalization on recently formed phagosomes (Fig. 6 B, boxed area 2). The Lamp1 patches detected in association with Syt VII–positive peripheral phagosomes (Fig. 6 B, boxed area 1) are likely to correspond to the highly dynamic Lamp1 tubules observed by live microscopy (Fig. 6 A, insets in frame at 3 min 12 s; and initial frames of Videos 2 and 3). Immunogold EM also detected endogenous (Fig. 7, A–C) or YFP-tagged (Fig. 7, D and E) Syt VII on tubular structures closely associated with Lamp1-containing compartments and endogenous Syt VII and Lamp1 on the membrane surrounding recently ingested zymosan particles (Fig. 7, F and G). Although Syt VII and Lamp1were apparently present on contiguous membrane segments, Syt VII was predominantly detected in clusters that appeared to exclude Lamp1 (Fig. 7, A–G; arrows). Together with the rapid recruitment of Syt VII to sites of phagosome and macropinosome formation, these observations suggest that Syt VII–containing microdomains on late endosomal/lysosomal compartments of BMMs may have unique properties that favor their rapid mobilization to the cell surface.

Quantitative image analysis reinforced the conclusion that Syt VII is mobilized to phagosomes from intracellular lysosomal compartments and not from the plasma membrane. The density of Syt VII–YFP on the phagosomal membrane relative to its density at the plasma membrane was measured on confocal images of BMMs fixed after 10 min of exposure to IgG-opsonized zymosan particles (Fig. 8 A). The density of CD11b, which was determined after staining with specific antibodies, was similar on the plasma membrane and on phagosomes. In 206 phagosomes examined, the mean CD11b phagosome/plasma membrane ratio was 1.19, confirming that phagosome maturation during this period was negligible. In contrast, Syt VII–YFP was significantly enriched in relation to the plasma membrane on 81% of the phagosomes (Fig. 8 B). Although the transient nature of plasma membrane ruffles did not allow a

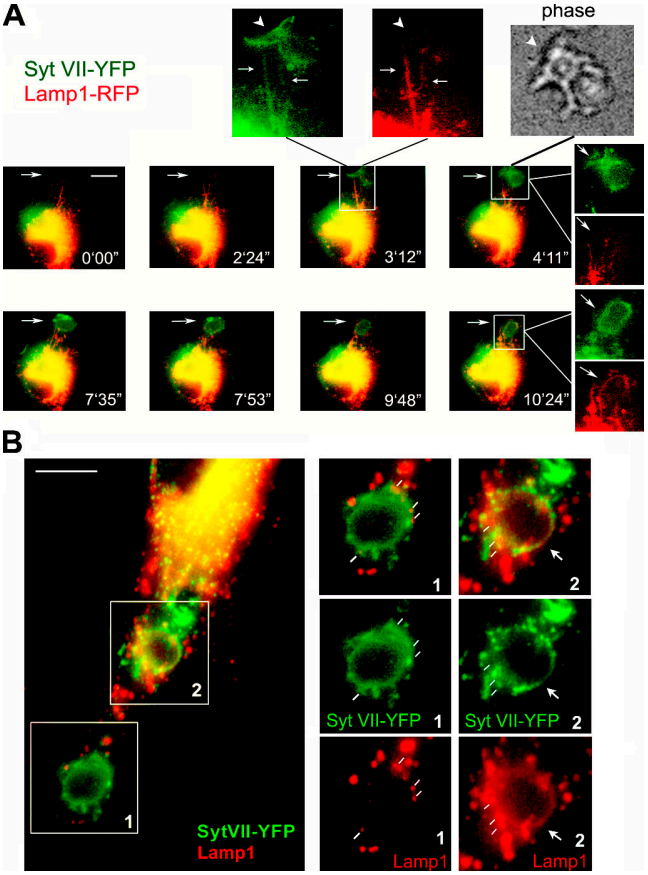

Figure 6. **Syt VII–YFP and Lamp1-RFP are sequentially delivered from tubular lysosomes to nascent phagosomes.** (A) Selected frames from a wide-field time-lapse video of a BMM transduced with Syt VII–YFP and Lamp1-RFP and exposed to 10 IgG-opsonized zymosan particles/cell (Videos 2–4, available at http://www.jcb.org/cgi/content/full/jcb.200605004/DC1). Frames from 0 min 0 s to 3 min 12 s: initial colocalization of Syt VII–YFP and Lamp1-RFP on tubular lysosomes expanding toward a site of phagosome formation. The arrow on the merged image at 3 min 12 s points to the boxed area reproduced in the enlarged, dissociated images above. Arrows point to tubular lysosomes containing both markers, and arrowheads point to Syt VII–YFP recruited to phagocytic cups (phase-contrast image, top). In the subsequent time points, Lamp1-containing tubules are seen wrapping themselves around Syt VII–YFP-containing phagosomes (frames from 7 min 35 s to 10 min 24 s; Videos 2–4). Dissociated, enlarged images are indicated by white lines originating from the merged image. Arrows point to the site of zymosan uptake. (B) Confocal microscopy images of BMMs transduced with Syt VII–YFP, exposed to IgG-opsonized zymosan for 20 min, fixed, and stained with anti-Lamp1 mAbs (red). In the same BMMs, two patterns of Lamp1 association with phagosomes can be seen (right). (1) Lamp1 patches (white lines) in close association with Syt VII–YFP-containing phagosomes (patches are likely to correspond to Lamp1 tubules surrounding the phagosome; A). (2) Lamp1 and Syt VII–YFP fully colocalize on the phagosome membrane (arrows). Bars (A), 10 μm; (B) 5 μm.

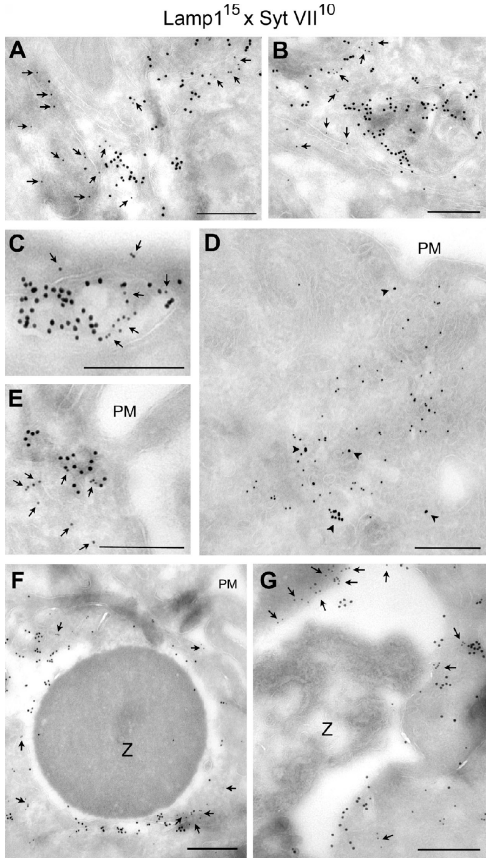

Figure 7. **Syt VII and Lamp1 are localized on distinct microdomains of tubulovesicular lysosomes and phagosomes.** (A–C) Immunogold labeling of BMM ultrathin cryosections detected endogenous Syt VII and Lamp1 on apparently contiguous microdomains of tubulovesicular compartments. 15 nm gold, mAbs to Lamp1; 10 nm gold, antibodies to Syt VII. (D and E) Immunogold labeling of Syt VII–YFP in transduced BMMs showing that its distribution is similar to the endogenous protein (associated with Lamp1 on peripheral tubulovesicular compartments). 15 nm gold, mAbs to Lamp1; 10 nm gold, anti-GFP antibodies. In A, B, C, and E, the arrows point to gold particles labeling Syt VII; in D, the arrowheads point to gold particles labeling Lamp1. (F and G) Immunogold detection of endogenous Syt VII and Lamp1 on microdomains of recently formed phagosomes (BMMs were incubated with IgG-opsonized zymosan for 10 min). In F, the ruffling plasma membrane is visible on the top right (PM). Arrows point to gold particles detecting Syt VII on phagosome-associated membranes. 15 nm gold, mAbs to Lamp1; 10 nm gold, antibodies to Syt VII. Z, zymosan particle. Bars (A–E), 200 nm; (F and G) 400 nm.

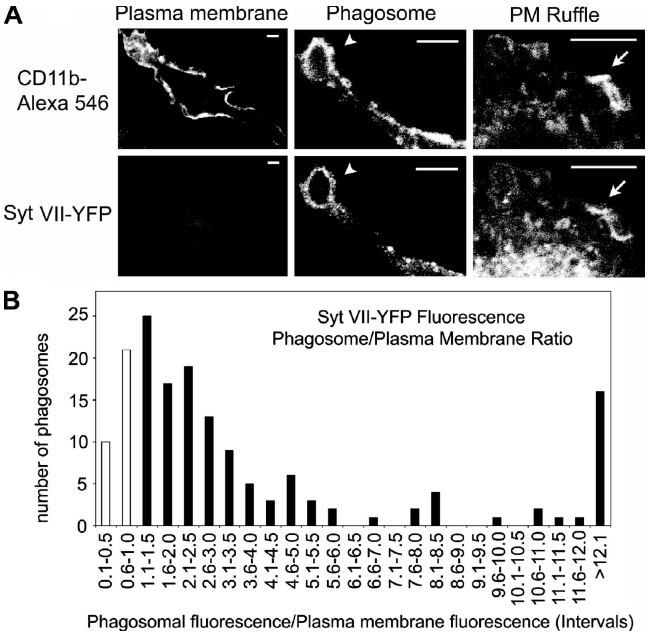

Figure 8. **Syt VII–YFP-containing intracellular compartments contribute to phagosome formation.** (A) Representative confocal images of anti-CD11b–AlexaFluor546 antibodies or Syt VII–YFP on the plasma membrane, phagosomes (arrowheads), and plasma membrane ruffles (arrows) of transduced BMMs. Bars, 5 μm. (B) Quantitation of the relative fluorescence intensity of Syt VII–YFP on 206 phagosomes. Each bar represents the number of phagosomes with a phagosome/plasma membrane fluorescence ratio within the intervals indicated. Black bars, phagosomes (81% of the total) in which Syt VII–YFP was enriched in relation to the plasma membrane (ratio of >1). White bars, phagosomes showing a ratio of <1. Data were normalized to the fluorescence intensity of the plasma membrane of the same cell.

more extensive quantitative analysis, Syt VII–YFP also appeared to be enriched on areas of active plasma membrane ruffling (Fig. 8 A).

Discussion

In this study, we showed that primary macrophages lacking the lysosomal Ca^{2+} sensor Syt VII are defective in the phagocytosis of large particle loads. This defect is independent of the receptor used for phagocytosis and can be rescued by the expression of wild-type Syt VII. Imaging of particle uptake revealed that Syt VII is localized on discrete, dynamic domains of the highly tubular lysosomal compartment of macrophages (Swanson et al., 1987). Syt VII is rapidly mobilized from these domains to nascent phagosomes, which shortly thereafter also acquire the abundant lysosomal glycoprotein Lamp1. Indicating a direct role for Syt VII in regulating lysosomal membrane delivery to phagocytic cups, Lamp1 detection on recently formed phagosomes was markedly reduced in Syt $VII^{-/-}$ BMMs. Several lines of evidence indicate that the early lysosomal membrane delivery observed in our studies is not a consequence of phagosome maturation (Lang et al., 1988; Desjardins et al., 1994). First, during the short particle uptake period used in these assays (10 min), the density of the plasma membrane protein CD11b remained constant on phagosomes and the plasma membrane (mean ratio of 1.19). Second, the large majority of phagosomes formed during this period were still surrounded by polymerized actin and were frequently observed close to the cell surface. Third, a detailed study of phagosome maturation was previously performed with cells from Syt $VII^{-/-}$ mice and revealed no defects in the uptake, transport, and lysosomal degradation of EGF and in the uptake and intralysosomal killing of *E. coli* (Roy et al., 2004).

Mutations abolishing the Ca^{2+}-dependent membrane association activity of Syt VII also abolished its ability to restore phagocytosis in Syt VII–null macrophages. The fact that Syt VII is a Ca^{2+}-binding protein that regulates the fusion of lysosomes with the plasma membrane (Martinez et al., 2000; Reddy et al., 2001; Chakrabarti et al., 2003) raised the possibility that the delivery of lysosomal membrane might correspond to a Ca^{2+}-dependent supplemental source of membrane during phagocytosis.

Consistent with this view, we found that the chelation of $[Ca^{2+}]_i$ inhibited phagocytosis in wild-type BMMs to a significantly larger extent when compared with the inhibition observed under the same conditions in Syt VII$^{-/-}$ BMMs. It has long been known that the ligation of phagocytic receptors, particularly the macrophage FcγR, triggers transient increases in $[Ca^{2+}]_i$ (Young et al., 1984). In neutrophils, intracellular Ca^{2+} stores seem to redistribute around sites of phagocytosis (Stendahl et al., 1994), emphasizing the apparently important role played by $[Ca^{2+}]_i$ in particle uptake. However, the requirement of Ca^{2+} signaling for phagocytosis in macrophages has remained controversial. Some studies concluded that the chelation of intracellular Ca^{2+} had no effect on the uptake of IgG-opsonized particles (Di Virgilio et al., 1988; Greenberg et al., 1991), whereas others reported a marked inhibition in phagocytosis (Young et al., 1984; Hishikawa et al., 1991). Our present study clarifies this issue by demonstrating that $[Ca^{2+}]_i$ transients and Syt VII–mediated lysosome recruitment are required for phagosome formation, but only under conditions of high membrane demand. The experimental conditions of studies in which $[Ca^{2+}]_i$ transients were found not to play a role may have favored uptake pathways that were not dependent on Syt VII–mediated mobilization of lysosomal membrane (Di Virgilio et al., 1988; Greenberg et al., 1991).

Although nascent phagosomes are formed in large part by invagination of the plasma membrane (Silverstein et al., 1977), it became evident in recent years that intracellular compartments also contribute to the process. Intracellular membrane is delivered to the cell surface during phagocytosis (Hackam et al., 1998; Holevinsky and Nelson, 1998), and functional inhibition of the exocytosis of VAMP3-containing early endosomes (Hackam et al., 1998; Bajno et al., 2000; Cox et al., 2000) or VAMP7-containing late endosomes/lysosomes (Braun et al., 2004) inhibits particle uptake. The endoplasmic reticulum was also proposed as a source of phagosomal membrane (Gagnon et al., 2002), but more recent studies failed to confirm that this is a widespread process, particularly during the uptake of IgG-opsonized particles (Henry et al., 2004; Touret et al., 2005). Our present studies are fully consistent with recent evidence implicating lysosomes as an important source of membrane during phagocytosis (Braun et al., 2004). Our results expand those findings by showing that the delivery of lysosomal membrane is dependent on the Ca^{2+} sensor Syt VII and, thus, is likely to correspond to a Ca^{2+}-sensitive component of the phagocytic process. Our findings are also consistent with additional observations from other laboratories, which have reported an early fusion of lysosomes with phagosomes containing *Candida albicans* (Kaposzta et al., 1999) and the rapid wrapping of lysosomal tubules around nascent phagosomes in mouse BMMs (Knapp and Swanson, 1990). These results suggest that the remarkable ability of macrophages to engulf daunting particle loads may be largely attributed to the Syt VII/Ca^{2+}-dependent use of lysosomes as a supplemental source of membrane.

Early endosome and lysosome membrane delivery appear to be tightly coordinated during phagosome formation, with the recruitment of VAMP7 immediately following the accumulation of the early endosome SNARE VAMP3 (Braun et al., 2004). In our study, Syt VII was detected on late endosomal/lysosomal membrane domains proximal to the plasma membrane but was not associated with transferrin-containing early endosomes. Interestingly, in RAW264.7 macrophages, VAMP7 was also detected at more peripheral domains of Lamp1-positive lysosomes (Braun et al., 2004). These observations suggest that the lysosomal compartments of macrophages may contain specialized microdomains containing both a Ca^{2+} sensor (Syt VII) and a fusogenic SNARE (VAMP7) at a peripheral location that facilitates rapid fusion with the plasma membrane.

Syt VII was also mobilized to sites of plasma membrane ruffling and to macropinosomes, which is consistent with the fact that the phagocytosis defect of Syt VII$^{-/-}$ BMMs is receptor independent. This finding suggests an intriguing coupling between signaling events leading to rearrangements of the cortical cytoskeleton and the rapid fusion of Syt VII–containing lysosomal microdomains with the plasma membrane. PI 3-kinase–generated phosphoinositol phosphates have been extensively linked to membrane traffic events and to actin remodeling (Toker and Cantley, 1997). Thus, it is noteworthy that treatment of macrophages with the PI 3-kinase inhibitor wortmannin generates a phenotype that is very similar to the genetic ablation of Syt VII: phagocytosis is inhibited proportionally to an increase in the size of the particles (Cox et al., 1999). Further analysis of the highly dynamic Syt VII–containing microdomains of macrophage lysosomes should provide useful insights into this process. Syt VII was previously shown to be involved in plasma membrane repair (Reddy et al., 2001; Chakrabarti et al., 2003) and in neurite extension by primary sympathetic neurons (Arantes and Andrews, 2006), suggesting that intracellular signaling domains containing this Ca^{2+} sensor may control several plasma membrane–remodeling events in addition to phagocytosis.

Materials and methods

Cell culture

Mouse BMMs were prepared from C57BL/6 wild-type (Syt VII$^{+/+}$) and Syt VII$^{-/-}$ mice (backcrossed into the C57BL/6 background; Chakrabarti et al., 2003) as previously described (Roy et al., 2004), seeded onto 96- (100 μl of a 5×10^5 BMM/ml suspension) or 24-well (0.5 ml of a 1.5×10^5 BMM/ml suspension) plates 24 h before experiments, and incubated in BMM media (RPMI, 10% FBS, 20% L cell–conditioned supernatant, and 1% penicillin/streptavidin) at 37°C and 5% CO_2.

Phagocytosis assays

Zymosan. Zymosan red bioparticles (Invitrogen) were opsonized by incubation with purified rabbit polyclonal IgG-opsonizing reagent (Invitrogen) for 1 h at 37°C as recommended by the manufacturer. BMMs were incubated with opsonized zymosan red at different particle/cell ratios for different periods of time, washed four times with PBS, and the fluorescence was read in a fluorimeter (Spectra MAX GEMINI; Invitrogen) at 595/620 nm. Background absorbance levels corresponding to wells containing BMMs alone were subtracted from all values. The cell number on each well was subsequently determined by lysing the cells in 1% Triton X-100 and assaying for lactate dehydrogenase activity (CytoTox 96 Non-radioactive Cytotoxicity Assay; Promega). These assays indicated that no cell loss occurred during the experiments. For calcium chelation assays, BMMs were incubated in HBSS without calcium and magnesium chloride containing 100 μM BAPTA-AM (Invitrogen) and 5 mM EGTA for 30 min at room temperature before incubation with opsonized zymosan.

Polystyrene particles. Yellow fluorescent particles (Spherotech) of different diameters (3 and 6 μm) were opsonized by incubating 10^8 particles/ml for 30 min at room temperature with 15 μg/ml of goat Fc-specific anti–mouse IgG (Sigma-Aldrich). BMMs were incubated with opsonized particles

at different ratios for different periods of time, washed four times with PBS, and the fluorescence was read at 488/530 nm.

Sheep RBCs. 10^8 sheep RBCs (MP Biomedicals) were washed twice with PBS and opsonized for 30 min at room temperature with 15 μg/ml of rabbit anti–sheep RBC IgG (MP Biomedicals) or rabbit anti–sheep RBC IgM (Accurate) antibodies. IgM-opsonized sheep RBCs were further incubated with 10% C5-deficient human complement (Sigma-Aldrich) for 20 min at 37°C. After opsonization, sheep RBCs were washed twice with PBS and resuspended in prewarmed BMM media. Before incubation with complement-opsonized sheep RBCs, BMMs were preincubated with 150 ng/ml PMA (Sigma-Aldrich) for 15 min at 37°C. BMMs were then incubated for various periods of time with opsonized sheep RBCs at an RBC/macrophage ratio of 10:1. After incubation, cells were washed three times with PBS and fixed in 2% PFA overnight at 4°C.

For microscopy-based assays, macrophages incubated with zymosan red were fixed with 2% PFA and stained with a 1:250 dilution of goat anti–rabbit IgG AlexaFluor488 (Invitrogen) without permeabilization to stain extracellular particles. For the detection of extracellular polystyrene particles, rabbit anti–goat IgG AlexaFluor546 (Invitrogen) was used at a 1:200 dilution. For the detection of extracellular IgG-coated sheep RBCs, goat anti–rabbit IgG AlexaFluor488 was used at a dilution of 1:250. To detect noninternalized C3bi-opsonized sheep RBCs, mouse anti–rabbit IgM-FITC (Sigma-Aldrich) was used at a dilution of 1:100. Approximately 300–350 BMMs were analyzed for each condition.

Flow cytometry

Flow cytometry was performed in a flow cytometer (FacsCalibur; Becton Dickinson) to quantify the amount of surface-exposed FcγR or CR3 (CD11b) receptors in Syt VII$^{+/+}$ and VII$^{-/-}$ BMMs. 10^6 BMMs were kept in suspension on ice for 20 min in PBS and 2% BSA followed by staining with 5 μg/ml FITC-conjugated rat anti–mouse CD16/CD32 (Fcg III/II receptor) mAbs (BD Biosciences) or 5 μg/ml rat anti–mouse CD11b (integrin α_M chain Mac1) antibodies (BD Biosciences), secondary goat anti–rat AlexaFluor488-conjugated antibodies (Invitrogen) for 20 min on ice, washes, resuspension in 1 ml PBS, and FACS analysis.

Fluorescence labeling, imaging, and image analysis

For Lamp1 detection, PFA-fixed BMMs were permeabilized with 0.2% saponin and stained with 1D4b anti–mouse Lamp1 mAbs (Developmental Studies Hybridoma Bank) followed by secondary anti–rat IgG AlexaFluor568 or -488 antibodies (Invitrogen). Phalloidin staining of phagosomes was performed on BMMs incubated for 10 min with 50 IgG-opsonized zymosan red particles/cell, washed, PFA fixed, permeabilized with 0.05% Triton X-100 for 5 min, and labeled with 0.1 μg/ml phalloidin-FITC (Sigma-Aldrich) for 20 min. For detection of the plasma membrane marker CD11b, PFA-fixed BMMs were permeabilized with 0.5% saponin and labeled with 10 μg/ml of rat anti–mouse CD11b antibodies (Becton Dickinson) followed by secondary anti–rat IgG AlexaFluor546 antibodies. For the detection of dextran-loaded lysosomes, BMMs were incubated with 0.25 mg/ml lysine-fixable rhodamine B–dextran (10 kD; Invitrogen) for 1 h at 37°C, washed, and chased in fresh medium for 2–3 h followed by fixation. For the detection of transferrin-containing early endosomes, BMMs were incubated with 50 μg/ml AlexaFluor555-transferrin (Invitrogen) for 1 h at 37°C followed by fixation.

Images were acquired using a microscope (Axiovert; Carl Zeiss MicroImaging, Inc.) through a 100× objective using a cooled CCD camera (Orca II; Hamamatsu) controlled by MetaMorph software (Universal Imaging Corp.) or a laser scanning confocal microscope (z-stack images were acquired with optical sections of 0.5–0.8 μm at 1-μm intervals; LSM 510; Carl Zeiss MicroImaging, Inc.). For quantitative image analysis, images were imported into ImageJ (National Institutes of Health [NIH]; http://rsb.info.nih.gov/ij/), and the mean fluorescence per pixel was measured using the measurement tool. For the quantitation of lysosome fusion with phagosomes containing zymosan, for each condition, >200 phagosomes were counted in a blinded fashion by two independent investigators. For quantitation of phalloidin staining, 350 phagosomes were counted for each condition (Syt VII$^{+/+}$ and VII$^{-/-}$ BMMs).

Retroviral transduction and live imaging

Bone marrow–derived progenitor cells were transduced using retroviral vectors encoding Lamp1-RFP (pLZRS-Lamp1-RFP), Syt VII–YFP (pLZRS-SytVII-YFP), or CFP-CD63 (pLZRS-CFP-CD63) with virus generation as previously described (Sherer et al., 2003). pLZRS-Lamp1-RFP was prepared by swapping the coding region GFP with RFP using BamHI–NotI sites in the retroviral construct pLZRS-EGFP-NL-lgp120 (a gift from J. Lippincott-Schwartz, NIH, Bethesda, MD; Patterson and Lippincott-Schwartz, 2002). Syt VII–YFP and CFP-CD63 were constructed by insertion of the Syt VII or CD63 coding regions from Syt VII–GFP (Martinez et al., 2000) or GFP-CD63 (Blott et al., 2001) into modified pLZRS-CFP or -YFP retroviral constructs using XhoI and HindIII sites. For retroviral transduction, 4×10^6 cells were incubated with viral supernatants 1 d after isolation at 4°C for 1–2 h before plating on 9-cm nontissue culture-treated dishes (Falcon). To improve transduction efficiency, additional aliquots of viral supernatant were added to the differentiating BMM cultures on days 2 and 3 after isolation.

Live imaging of zymosan uptake was performed on a heated stage using the 100× NA 1.4 objective of a laser scanning confocal microscope (LSM 510; Carl Zeiss MicroImaging, Inc,) or the 60× NA 1.4 objective of an epifluorescent microscope (TE2000; Nikon). For wide-field time-lapse videos, YFP and RFP channels were imaged simultaneously every 15–60 s. All videos were saved as QuickTime files and were compressed and edited using Sorenson Squeeze 4 (Sorenson Media), Openlab (Improvision), or Photoshop software (Adobe).

Immunogold labeling and EM

BMMs transduced or untransduced with Syt VII–YFP were incubated with 50 IgG-opsonized zymosan particles per cell for 10 min at 37°C, washed three times with PBS, and fixed with 4% PFA in 0.25 M Hepes, pH 7.4, for 1 h at room temperature followed by an overnight fixation in 8% PFA in the same buffer at 4°C. After washes in PBS, cells were scraped, embedded in 10% gelatin, infiltrated overnight in 2.3 M sucrose, and frozen in liquid nitrogen. Ultrathin frozen sections were double labeled with anti-GFP, anti–Syt VII (Arantes and Andrews, 2006), and anti-Lamp1 antibodies using previously described methods (Folsch et al., 2003). Sections were examined in an electron microscope (Tecnai 12 Biotwin; FEI), and images were captured digitally using a CCD camera (Morada; Soft Imaging Systems).

Site-directed mutagenesis, functional reconstitution assays, and Syt–PS-binding assays

D225,227,357,359N (designated as D/N) mutations that neutralize the putative Ca^{2+}-binding ligands in each C2 domain of Syt VII were introduced into the Syt VII–YFP plasmid using the QuikChange Site-Directed Mutagenesis Kit (Stratagene). After retroviral transduction with wild-type, mutated Syt VII–YFP, or vector alone, BMMs were incubated with 25 zymosan red particles/cell at 37°C for 1 h, and 400 BMMs were analyzed for each condition.

For Syt–PS-binding assays, cDNA encoding the cytoplasmic domain of Syt I (C2AB I, residues 96–421) and Syt VII (C2AB VII, residues 134–403) were subcloned into pGEX-2T vector (GE Healthcare). D/N corresponds to mutations that neutralize the putative Ca^{2+}-binding ligands in each C2 domain (D230,232,363,365N for C2AB I and D225,227, 357,359N for C2AB VII). Proteins were expressed as GST fusion proteins and purified using glutathione–Sepharose beads (GE Healthcare) as described previously (Chapman et al., 1995; Bhalla et al., 2006). Synthetic 1,2-dioleoyl-*sn*-glycero-3-phospho-L-serine (PS), 1,2-dioleoyl-*sn*-glycero-3-phosphocholine (PC), and *N*-(lissamine rhodamine B sulfonyl)-1, 2-dipalmitoyl-*sn*-glycero-3-phosphoethanolamine were purchased from Avanti Polar Lipids, Inc. Large (~100 nm) unilamellar liposomes were prepared by extrusion as described previously (Davis et al., 1999). Liposomes were composed of 1% *N*-(lissamine rhodamine B sulfonyl)-1,2-dipalmitoyl-*sn*-glycero-3-phosphoethanolamine, 25% PS, and 74% PC. Syt–PS interactions were measured by using rhodamine-labeled liposome pull-down assays as described previously (Hui et al., 2005). Immobilized proteins and liposomes were coincubated in binding buffer plus 2 mM EGTA or 0.2 mM Ca^{2+} in Micro Bio-Spin chromatography columns (Bio-Rad Laboratories) for 15 min at room temperature. Samples were then rapidly washed three times with their respective binding buffers. Bound liposomes were eluted with Hepes buffer containing 1% Triton X-100. The extent of binding was determined by measuring the fluorescence intensity of rhodamine in the eluate.

Online supplemental material

Fig. S1 shows that Syt VII$^{-/-}$ mouse BMMs do not have a reduced expression of surface receptors for IgG or complement. Fig. S2 shows immunogold EM localization of Lamp1 on a recently formed phagosome containing zymosan. The videos show that Syt VII–YFP expressed in a wild-type macrophage is delivered to nascent phagosomes during the uptake of zymosan particles. The macrophage shown in Videos 2–4 was also transduced with Lamp1-RFP. This marker is visualized on tubular lysosomes extending toward the site of zymosan uptake and surrounding recently formed phagosomes. Online supplemental material is available at http://www.jcb.org/cgi/content/full/jcb.200605004/DC1.

We are grateful to Henry Tan for help with figure preparation.

This work was supported by NIH grants RO1GM064625 and R37AI34867 to N.W. Andrews, NIH grant RO1CA098727 to W. Mothes, and National Institute of General Medical Sciences grant GM56827 and National Institute of Mental Health grant MH61876 to E.R. Chapman.

Submitted: 1 May 2006
Accepted: 17 August 2006

References

Aderem, A., and D.M. Underhill. 1999. Mechanisms of phagocytosis in macrophages. *Annu. Rev. Immunol.* 17:593–623.

Advani, R.J., H.R. Bae, J.B. Bock, D.S. Chao, Y.C. Doung, R. Prekeris, J.S. Yoo, and R.H. Scheller. 1998. Seven novel mammalian SNARE proteins localize to distinct membrane compartments. *J. Biol. Chem.* 273:10317–10324.

Advani, R.J., B. Yang, R. Prekeris, K.C. Lee, J. Klumperman, and R.H. Scheller. 1999. VAMP-7 mediates vesicular transport from endosomes to lysosomes. *J. Cell Biol.* 146:765–776.

Arantes, R.M., and N.W. Andrews. 2006. A role for synaptotagmin VII-regulated exocytosis of lysosomes in neurite outgrowth from primary sympathetic neurons. *J. Neurosci.* 26:4630–4637.

Bajno, L., X.R. Peng, A.D. Schreiber, H.P. Moore, W.S. Trimble, and S. Grinstein. 2000. Focal exocytosis of VAMP3-containing vesicles at sites of phagosome formation. *J. Cell Biol.* 149:697–706.

Bhalla, A., W. Tucker, and E.R. Chapman. 2005. Synaptotagmin isoforms couple distinct ranges of Ca2+, Ba2+, and Sr2+ concentration to SNARE-mediated membrane fusion. *Mol. Biol. Cell*. 16:4755–4764.

Bhalla, A., M.C. Chicka, W.C. Tucker, and E.R. Chapman. 2006. Ca(2+)-synaptotagmin directly regulates t-SNARE function during reconstituted membrane fusion. *Nat. Struct. Mol. Biol*. 13:323–330.

Blott, E.J., G. Bossi, R. Clark, M. Zvelebil, and G.M. Griffiths. 2001. Fas ligand is targeted to secretory lysosomes via a proline-rich domain in its cytoplasmic tail. *J. Cell Sci.* 114:2405–2416.

Braun, V., V. Fraisier, G. Raposo, I. Hurbain, J.B. Sibarita, P. Chavrier, T. Galli, and F. Niedergang. 2004. TI-VAMP/VAMP7 is required for optimal phagocytosis of opsonised particles in macrophages. *EMBO J.* 23:4166–4176.

Caler, E.V., S. Chakrabarti, K.T. Fowler, S. Rao, and N.W. Andrews. 2001. The exocytosis-regulatory protein Synaptotagmin VII mediates cell invasion by *Trypanosoma cruzi*. *J. Exp. Med.* 193:1097–1104.

Chakrabarti, S., K.S. Kobayashi, R.A. Flavell, C.B. Marks, K. Miyake, D.R. Liston, K.T. Fowler, F.S. Gorelick, and N.W. Andrews. 2003. Impaired membrane resealing and autoimmune myositis in synaptotagmin VII-deficient mice. *J. Cell Biol.* 162:543–549.

Chapman, E.R. 2002. Synaptotagmin: a Ca(2+) sensor that triggers exocytosis? *Nat. Rev. Mol. Cell Biol.* 3:498–508.

Chapman, E.R., P.I. Hanson, S. An, and R. Jahn. 1995. Ca2+ regulates the interaction between synaptotagmin and syntaxin 1. *J. Biol. Chem.* 270:23667–23671.

Cox, D., C.C. Tseng, G. Bjekic, and S. Greenberg. 1999. A requirement for phosphatidylinositol 3-kinase in pseudopod extension. *J. Biol. Chem.* 274:1240–1247.

Cox, D., D.J. Lee, B.M. Dale, J. Calafat, and S. Greenberg. 2000. A Rab11-containing rapidly recycling compartment in macrophages that promotes phagocytosis. *Proc. Natl. Acad. Sci. USA*. 97:680–685.

Davis, A.F., J. Bai, D. Fasshauer, M.J. Wolowick, J.L. Lewis, and E.R. Chapman. 1999. Kinetics of synaptotagmin responses to Ca2+ and assembly with the core SNARE complex onto membranes. *Neuron*. 24:363–376.

Desjardins, M., L.A. Huber, R.G. Parton, and G. Griffiths. 1994. Biogenesis of phagolysosomes proceeds through a sequential series of interactions with the endocytic apparatus. *J. Cell Biol.* 124:677–688.

Di Virgilio, F., B.C. Meyer, S. Greenberg, and S.C. Silverstein. 1988. Fc receptor-mediated phagocytosis occurs in macrophages at exceedingly low cytosolic Ca2+ levels. *J. Cell Biol.* 106:657–666.

Duffield, A., E.J. Kamsteeg, A.N. Brown, P. Pagel, and M.J. Caplan. 2003. The tetraspanin CD63 enhances the internalization of the H,K-ATPase beta-subunit. *Proc. Natl. Acad. Sci. USA*. 100:15560–15565.

Earles, C.A., J. Bai, P. Wang, and E.R. Chapman. 2001. The tandem C2 domains of synaptotagmin contain redundant Ca2+ binding sites that cooperate to engage t-SNAREs and trigger exocytosis. *J. Cell Biol.* 154:1117–1123.

Folsch, H., M. Pypaert, S. Maday, L. Pelletier, and I. Mellman. 2003. The AP-1A and AP-1B clathrin adaptor complexes define biochemically and functionally distinct membrane domains. *J. Cell Biol.* 163:351–362.

Fukuda, M., E. Kanno, M. Satoh, C. Saegusa, and A. Yamamoto. 2004. Synaptotagmin VII is targeted to dense-core vesicles and regulates their Ca2+-dependent exocytosis in PC12 cells. *J. Biol. Chem.* 279:52677–52684.

Gagnon, E., S. Duclos, C. Rondeau, E. Chevet, P.H. Cameron, O. Steele-Mortimer, J. Paiement, J.J. Bergeron, and M. Desjardins. 2002. Endoplasmic reticulum-mediated phagocytosis is a mechanism of entry into macrophages. *Cell*. 110:119–131.

Gao, Z., J. Reavey-Cantwell, R.A. Young, P. Jegier, and B.A. Wolf. 2000. Synaptotagmin III/VII isoforms mediate Ca2+-induced insulin secretion in pancreatic islet beta-cells. *J. Biol. Chem.* 275:36079–36085.

Greenberg, S., and S. Grinstein. 2002. Phagocytosis and innate immunity. *Curr. Opin. Immunol.* 14:136–145.

Greenberg, S., J. el Khoury, F. di Virgilio, E.M. Kaplan, and S.C. Silverstein. 1991. Ca(2+)-independent F-actin assembly and disassembly during Fc receptor-mediated phagocytosis in mouse macrophages. *J. Cell Biol.* 113:757–767.

Hackam, D.J., O.D. Rotstein, C. Sjolin, A.D. Schreiber, W.S. Trimble, and S. Grinstein. 1998. v-SNARE-dependent secretion is required for phagocytosis. *Proc. Natl. Acad. Sci. USA*. 95:11691–11696.

Hakansson, A., C.C. Bentley, E.A. Shakhnovic, and M.R. Wessels. 2005. Cytolysin-dependent evasion of lysosomal killing. *Proc. Natl. Acad. Sci. USA*. 102:5192–5197.

Henry, R.M., A.D. Hoppe, N. Joshi, and J.A. Swanson. 2004. The uniformity of phagosome maturation in macrophages. *J. Cell Biol.* 164:185–194.

Hishikawa, T., J.Y. Cheung, R.V. Yelamarty, and D.W. Knutson. 1991. Calcium transients during Fc receptor-mediated and nonspecific phagocytosis by murine peritoneal macrophages. *J. Cell Biol.* 115:59–66.

Holevinsky, K.O., and D.J. Nelson. 1998. Membrane capacitance changes associated with particle uptake during phagocytosis in macrophages. *Biophys. J.* 75:2577–2586.

Hui, E., J. Bai, P. Wang, M. Sugimori, R.R. Llinas, and E.R. Chapman. 2005. Three distinct kinetic groupings of the synaptotagmin family: candidate sensors for rapid and delayed exocytosis. *Proc. Natl. Acad. Sci. USA*. 102:5210–5214.

Jaiswal, J.K., N.W. Andrews, and S.M. Simon. 2002. Membrane proximal lysosomes are the major vesicles responsible for calcium-dependent exocytosis in nonsecretory cells. *J. Cell Biol.* 159:625–635.

Kaposzta, R., L. Marodi, M. Hollinshead, S. Gordon, and R.P. da Silva. 1999. Rapid recruitment of late endosomes and lysosomes in mouse macrophages ingesting *Candida albicans*. *J. Cell Sci.* 112:3237–3248.

Knapp, P.E., and J.A. Swanson. 1990. Plasticity of the tubular lysosomal compartment in macrophages. *J. Cell Sci.* 95:433–439.

Koh, T.W., and H.J. Bellen. 2003. Synaptotagmin I, a Ca2+ sensor for neurotransmitter release. *Trends Neurosci.* 26:413–422.

Lang, T., C. de Chastellier, A. Ryter, and L. Thilo. 1988. Endocytic membrane traffic with respect to phagosomes in macrophages infected with non-pathogenic bacteria: phagosomal membrane acquires the same composition as lysosomal membrane. *Eur. J. Cell Biol.* 46:39–50.

Leoni, P., and R.T. Dean. 1983. Mechanisms of lysosomal enzyme secretion by human monocytes. *Biochim. Biophys. Acta*. 762:378–389.

Li, C., B. Ullrich, J.Z. Zhang, R.G. Anderson, N. Brose, and T.C. Sudhof. 1995. Ca(2+)-dependent and -independent activities of neural and non-neural synaptotagmins. *Nature*. 375:594–599.

Martinez, I., S. Chakrabarti, T. Hellevik, J. Morehead, K. Fowler, and N.W. Andrews. 2000. Synaptotagmin VII regulates Ca(2+)-dependent exocytosis of lysosomes in fibroblasts. *J. Cell Biol.* 148:1141–1149.

McNeil, P.L., J.A. Swanson, S.D. Wright, S.C. Silverstein, and D.L. Taylor. 1986. Fc-receptor-mediated phagocytosis occurs in macrophages without an increase in average [Ca++]i. *J. Cell Biol.* 102:1586–1592.

Niedergang, F., E. Colucci-Guyon, T. Dubois, G. Raposo, and P. Chavrier. 2003. ADP ribosylation factor 6 is activated and controls membrane delivery during phagocytosis in macrophages. *J. Cell Biol.* 161:1143–1150.

Patterson, G.H., and J. Lippincott-Schwartz. 2002. A photoactivatable GFP for selective photolabeling of proteins and cells. *Science*. 297:1873–1877.

Pelchen-Matthews, A., B. Kramer, and M. Marsh. 2003. Infectious HIV-1 assembles in late endosomes in primary macrophages. *J. Cell Biol.* 162:443–455.

Reddy, A., E. Caler, and N. Andrews. 2001. Plasma membrane repair is mediated by Ca2+-regulated exocytosis of lysosomes. *Cell*. 106:157–169.

Roy, D., D.R. Liston, V.J. Idone, A. Di, D.J. Nelson, C. Pujol, J.B. Bliska, S. Chakrabarti, and N.W. Andrews. 2004. A process for controlling intracellular bacterial infections induced by membrane injury. *Science*. 304:1515–1518.

Sherer, N.M., M.J. Lehmann, L.F. Jimenez-Soto, A. Ingmundson, S.M. Horner, G. Cicchetti, P.G. Allen, M. Pypaert, J.M. Cunningham, and W. Mothes.

2003. Visualization of retroviral replication in living cells reveals budding into multivesicular bodies. *Traffic*. 4:785–801.

Silverstein, S.C., R.M. Steinman, and Z.A. Cohn. 1977. Endocytosis. *Annu. Rev. Biochem.* 46:669–722.

Stendahl, O., K.H. Krause, J. Krischer, P. Jerstrom, J.M. Theler, R.A. Clark, J.L. Carpentier, and D.P. Lew. 1994. Redistribution of intracellular Ca2+ stores during phagocytosis in human neutrophils. *Science*. 265:1439–1441.

Swanson, J., A. Bushnell, and S.C. Silverstein. 1987. Tubular lysosome morphology and distribution within macrophages depend on the integrity of cytoplasmic microtubules. *Proc. Natl. Acad. Sci. USA*. 84:1921–1925.

Tapper, H., and R. Sundler. 1995. Glucan receptor and zymosan-induced lysosomal enzyme secretion in macrophages. *Biochem. J.* 306:829–835.

Toker, A., and L.C. Cantley. 1997. Signalling through the lipid products of phosphoinositide-3-OH kinase. *Nature*. 387:673–676.

Touret, N., M. Paroutis, M. Terebiznik, R. Harrison, S. Trombetta, M. Pypaert, A. Chow, A. Jiang, J. Shaw, C. Yip, et al. 2005. Quantitative and dynamic assessment of the contribution of the ER to phagosome formation. *Cell*. 123:157–170.

Tucker, W.C., T. Weber, and E.R. Chapman. 2004. Reconstitution of Ca2+-regulated membrane fusion by synaptotagmin and SNAREs. *Science*. 304:435–438.

Wang, P., M.C. Chicka, A. Bhalla, D.A. Richards, and E.R. Chapman. 2005. Synaptotagmin VII Is targeted to secretory organelles in PC12 cells, where it functions as a high-affinity calcium sensor. *Mol. Cell. Biol.* 25:8693–8702.

Werb, Z., and Z.A. Cohn. 1972. Plasma membrane synthesis in the macrophage following phagocytosis of polystyrene latex particles. *J. Biol. Chem.* 247:2439–2446.

Werb, Z., and S. Gordon. 1975. Elastase secretion by stimulated macrophages. Characterization and regulation. *J. Exp. Med.* 142:361–377.

Young, J.D., S.S. Ko, and Z.A. Cohn. 1984. The increase in intracellular free calcium associated with IgG gamma 2b/gamma 1 Fc receptor-ligand interactions: role in phagocytosis. *Proc. Natl. Acad. Sci. USA*. 81:5430–5434.